Chapter 22
Airborne Remote Detection of Turbulence with Forward-Pointing LIDAR

Patrick Sergej Vrancken

Abstract Presently, the airborne remote detection of atmospheric turbulence is limited to radar-visible regions of the sky, i.e., zones that contain hydrometeors like rain or cloud droplets. The bulk of the actual turbulence, possible in clear air at all flight altitudes, evades such a remote detection, though a remote determination of aircraft-relevant physical parameters relevant to turbulence could significantly increase flight safety.

The following chapter reviews possible techniques of remote turbulence detection in clear air and identifies the most promising approaches for future aircraft. These are shown to be optical methods, i.e., LIDAR (Light Detection and Ranging) systems. Principles, as well as pros and cons of some complementary lidar techniques, are discussed.

22.1 Introduction

The forecasting of turbulent-prone zones in the aviation-relevant airspace is steadily making progress as was illustrated in Part III of this volume. Clear-air turbulence (CAT) occurrence is reported verbally by pilots or automatically by onboard in situ detection algorithms and can be used in upper-level turbulence nowcasting and forecasting applications. The understanding of turbulence induced by convective processes is improving, as is the nowcasting of the latter. High-resolution numerical weather prediction (NWP) domains around airports should allow more reliable prognosis of low-level turbulence and wind shear. Wake vortex behavior of nearby aircraft, from drift to dissolution, is increasingly well estimated.

For the coming decades, the aviation sector has set itself the goals of further improving the safety of passengers and crew, enhancing efficiency and timeliness, and increasing environmental sustainability and economic competitiveness (that

P.S. Vrancken (✉)
DLR – German Aerospace Center, Institute of Atmospheric Physics, Oberpfaffenhofen 82234, Germany
e-mail: Patrick.Vrancken@dlr.de

R. Sharman, T. Lane (eds.), *Aviation Turbulence*,
DOI 10.1007/978-3-319-23630-8_22

may both be supported by more lightweight, thus less fuel-consuming aircraft structures). Turbulence in the flightpath of an aircraft is a major obstacle in achieving these challenging goals, in particular in the context of the strong growth rate of global air traffic and climate change (see Chap. 23).

There are at least two aspects that emphasize the need of forecasts and nowcasts to be complemented with onboard remote sensing of turbulence. The first refers to the physical nature of turbulence that inherently shows intermittency and patchiness. Hence, turbulence does not occur at the large scales where it is forecasted, but locally, and temporarily. This results in vast volumes of airspace forecasted to develop turbulence, but it actually occurs in very localized, temporally varying areas wherever the physical conditions are favorable. The second, more operational aspect relates to the circumstance that often aircraft are constrained to follow a certain predefined route, be it through a CAT-prone area on a transatlantic trajectory over Greenland or during a wind shear-threatened approach to a specific airport. An appreciable deviation of a flight route due to a forecast may only be an alternative for very hazardous turbulent conditions since operational and economic aspects play an important role in commercial aviation. This is where the development of new remote sensing techniques comes in. As will be seen in this chapter, where the indispensable workhorse of aviation safety, the onboard weather radar, falls short due to its physical limitations, new optical techniques should hit the mark.

In the next sections we shall explore the two main applications of turbulence remote sensing. In order to understand the technological implications of remote detection of turbulence, we will shortly highlight the possible scope of such detection (Sect. 22.2) and the related physical observables (Sect. 22.3). A brief overview of forthcoming technologies (Sect. 22.4) shall clarify that many of them represent interesting research potential but should retain purely academic relevance. We will see that only active optical remote sensing (i.e., lidar) is a viable solution. In Sect. 22.5 lidar application to the problem is considered in more depth. From this description of lidar principles, we will deduce that there is still a substantial piece of technology and product development work to do that also relies on research into the actual physical peculiarities of turbulence (see Chap. 25). The aim of this chapter though is not to strictly detail lidar or any other technology since this information may be found elsewhere (e.g., Weitkamp 2005; Measures 1984 or cited references).

22.2 Aims of Turbulence Detection

There are two main areas of application of remote turbulence detection within aeronautics, depending on the actual range of detection: on long range to register evidence of turbulence along with information of intensity, i.e., around 15 km distance in order to give the flight crew or some automated system time to respond,

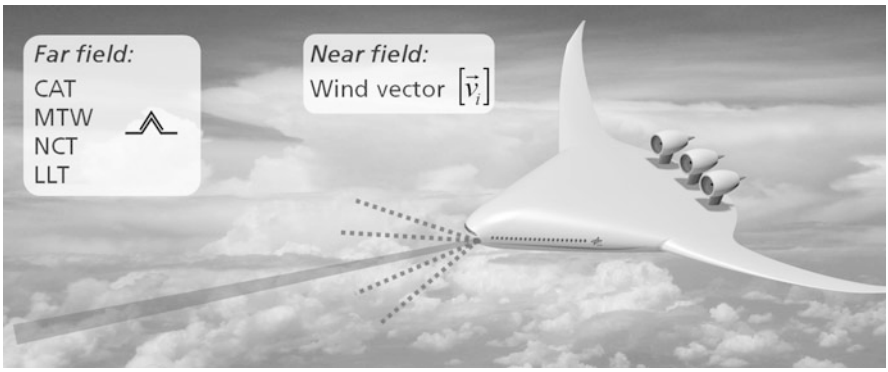

Fig. 22.1 Sketch highlighting the long-range and near-range application of remote turbulence sensing (Image: DLR CC-BY 3.0)

or on short range (some 50–150 m) to directly deliver wind vector information for automated action of the aircraft's control surfaces (see, e.g., Fig. 22.1).

The goal of long-range applications is to remotely detect the severity of turbulent motion of the air ahead with sufficient range to provide warning to the cockpit to take mitigating actions. Within clouds, state-of-the-art radar systems do this job and retrieve a measure of turbulence by analyzing the Doppler-broadened radar return. In clear air, outside clouds, where clear-air, mountain wave, and near-cloud turbulence occur, however, radar is blind to air motion due to the absence of backscattering hydrometeors. Arising in higher altitudes, this class of turbulence concerns the long cruise phase where crew and passengers stroll around the cabin and are thus susceptible to injuries in suddenly occurring turbulence. Further, the aircraft is typically flying at high speed which maximizes the loads and thus the induced bending moments in the wing roots (and consequently their fatigue). Turbulence also has an effect on the onset of high speed buffet and due to flying close to the edge of the envelope, which may lead to high speed stall. Here, a timely warning could alter the situation: from a simple seat belt sign for passenger safety, over mitigation actions such as deceleration, to evasion maneuvers. Anticipating the following section, the actual physical quantity representing the turbulence is of minor importance in this application as long as it reliably determines the presence and "strength" of the turbulent zone ahead, remembering that the most important quantity for an aircraft's disturbance is vertical wind speed.

The short-range application would comprise the determination of an actual wind speed vector, or a vector ensemble, resolved to fit the aircraft and turbulence characteristics. The aircraft's control system could thus determine and set the appropriate control actions of rudders and lift control devices in order to mitigate the induced moments and accelerations. Then, flying even through strong turbulence, the ride would be less bumpy, minimizing passenger and crew discomfort and any potential structural damage.

22.3 Turbulence Observables

Atmospheric turbulence relevant for aviation is characterized by chaotic deviations of wind velocity from its mean flow. Without focusing on the complex spectral characteristics, these fluctuations do occur on all spatial and temporal scales from the larger scales of generation (e.g., by shear due to jets or gravity waves) down to viscous dissipation on the mm to cm level. Regarding the remote detection of turbulence from fast-flying aircraft, and the resulting time interval between a detection ahead and the actual encounter, one may follow Taylor's hypothesis to consider the turbulence as "frozen," i.e., maintaining its characteristics over that time.

The important spatial scales for aviation, though, depend very much on the aircraft characteristics, such as size, weight, speed, and layout. The aircraft acts as a filter, damping high frequencies (by aerodynamics characteristics) and low wavenumbers of the large scales (e.g., through autopilot). From the encountered components[1] of the fluctuating wind velocity (u', v', and w'), the vertical component is the most important, with a tenfold stronger reaction in acceleration compared to the axial/horizontal wind speed fluctuations (Hoblit 1988). The w'- component would thus be the observable of choice for a distant warning, while its relationship to u' (and v') is neither simple nor universal due to anisotropy of the turbulence (e.g., Reiter and Burns 1966; Crooks et al. 1967; Lilly et al. 1973). In contrast we will see throughout the next sections that u' is basically the most accessible quantity (via Doppler shift measurement of backscattered radiation), v' practically immeasurable, and w' can only be determined with indirect methods (Sect. 22.5.3). The three fluctuating velocities may either be seen (directly) in the movement of the air molecules or of suspended particles (i.e., aerosols, ice crystals, water droplets). Over a certain range interval, they may be quantified by a statistical dispersion parameter such as its variance (e.g., $\sigma^2_{u'_{aer}}(R)$ for the fluctuation of head wind speed at distance R, determined from aerosol movement).

The air movement, on its part, generates fluctuations of its state variables temperature, T, and density, ρ, by the displacement and mixing of different atmospheric layers (thus $\sigma_T(R)$ and $\sigma_\rho(R)$). These in turn give rise to a second-order effect on the probing electromagnetic radiation: the variation of the air refractive index which depends on temperature, pressure, and humidity. It is generally quantified by its structure constant $C_n^2(R)$ which is proportional to the variance (multiplied with some length scale characterizing the turbulence).

In addition to the effect of mixing of the turbulent airflow on suspended particles (aerosols), it has a second effect on these passive "scalar" tracers: a certain structuring according to the spatial properties of the turbulent flow. Rather obvious

[1] We will henceforth consider an aircraft-fixed reference system, i.e., $u(R) = \overline{u}(R) + u'(R)$ be the velocity along the aircraft motion axis R, v' the lateral fluctuating component, and w' the vertical component.

and well proven for wake vortices (e.g., Misaka et al. 2012), such a mechanism is less evident for geophysically produced turbulence. The related observable would then be the spatial distribution of the respective scalar atmospheric constituent. However, considering the minute or absent effect on aerodynamics of the latter observables, a quantitative determination of aviation turbulence strength appears fairly precarious.

For now, we may stipulate that for our first aim, the long-range detection of turbulence for aviation the specific physical quantity is of lower importance. This is in contrast to a short-range flight control application where actual three-dimensional wind speed vectors have to be determined. In the following sections we will shortly discuss different technologies in order to determine the most promising ones that may enable future turbulence protection systems.

22.4 Technologies for Remote Detection of Turbulence

This section will give a short review of active remote sensing techniques that may provide information on the previously stated physical observables. Even though passive microwave radiometry had received some attention for airborne CAT detection in the 1960s, its shortcomings for operational use became rapidly evident (e.g., Atlas 1969; Schaffner et al. 2012). However, passive sensing techniques such as air temperature microwave radiometry (e.g., Haggerty et al. 2014) and star scintillation photometry (e.g., Vernin and Pelon 1986) could be valuable methods for determining ancillary scientific data in general experimental research on atmospheric turbulence.

Active remote sensing relies on the emission of electromagnetic radiation into the relevant region and collecting and analyzing the radiation that is backscattered from locally present objects. It generally allows a more robust determination of the aimed observable.

22.4.1 Radar Methods

Electromagnetic radiation in the microwave frequency region is effectively backscattered from hydrometeors such as cloud or rain droplets. The reflectivity is then a measure of liquid water content of the sensed volume ahead. The radar frequencies are chosen as a function of the application: ground-based precipitation radars operate at some GHz (S to C-Band) and modern airborne weather radars employ rather X-band (around 10 GHz). This makes the airborne radars very sensitive to clouds and rain while at the same time turns them essentially “blind” to anything behind very dense clouds (e.g., as occurring in deep convection). The choice of lower frequencies in ground-based systems allows them to more effectively sense through rain and dense clouds.

Scientific (Hamilton et al. 2012; Chap. 5) and state-of-the-art airborne weather radars (Baynes 2014) also exploit the Doppler information in order to determine the turbulence and/or wind shear in or around sufficiently reflecting air volumes (thus detecting in-cloud turbulence). However, such radar systems are not sensitive to anything other than water droplets. Therefore, flow information based on Doppler shift of the backscattered radiation is only available for these water-containing areas.

A different radar technique evaluates the backscatter of clear air. Bragg scatter occurring at successive refractive index and humidity perturbations (Clifford et al. 1994) leads to a coherent adding of the scattered wavefronts at the receiver. Thus, the backscattered radiation, quantified by the reflectivity η, is directly proportional to the refractive index variations $C^2_{n,\mathrm{Radar}}$ (i.e., the radar-optical turbulence intensity) divided by $\lambda_R^{1/3}$, the respective radar wavelength (Good et al. 1982; Ottersten 1969).

The reflectivity η is derived from the signal strength, or more precisely the signal-to-noise ratio (SNR) of the measurement. This technique is used in ground-based research on turbulence in the free atmosphere, employing VHF (30–300 MHz) or UHF (300 MHz–1 GHz) radar systems (e.g., Serafimovich et al. 2005; Luce et al. 2010) due to less atmospheric damping at lower frequencies. The drawback of this approach is the extremely low reflectivity; for instance, in common wind profilers it is typically ten orders of magnitude lower than for S-band weather radars that operate on backscatter on hydrometeors (Clifford et al. 1994). This yields very long integration times (>minutes) and challenges noise-processing algorithms. Further, the extended beam pattern (beam angle equals λ_R/D, with D antenna diameter) does not allow an altitude distinction precise enough for a reliable encounter prediction (of some tens to hundreds meters) in a hypothetic airborne horizontal application. Other inhibiting factors are the necessary size of the antenna, too bulky for aircraft integration, and range limitations due to ground echo. While some experimental effort has been carried out in the 1960s by the Boeing Company (Buehler et al. 1969), a thorough analysis of the relevant quantities' magnitudes (reflectivity, radar wavelength, achievable system parameters) shows the impracticality of a radar approach to airborne turbulence detection in clear air (Atlas et al. 1966; Watkins and Browning 1973).

Summarizing the radar approaches, it can be stated that the actually employed weather radar techniques, with all its possible evolutions, will continue to represent the most important airborne remote sensing instrument due to its ability to detect the chief weather hazards like deep convection along with its embedded wind shear and turbulence. Its limitation to these environments, though, demands a complementary system able to operate in dry and clear air.

22.4.2 THz Remote Sensing

For completeness, we shall mention here another remote sensing technique that is very sensitive to water vapor. THz radiation may effectively be employed to determine humidity and its variability. As conjectured in Sect. 22.3, one could ultimately derive the underlying turbulence from this variable. However, the very strong sensitivity toward water vapor at the same time also limits its applicable range whenever any humidity may be encountered. Therefore, its use in remote turbulence detection may be considered to remain marginal.

22.4.3 LIDAR: Light Detection and Ranging

Light Detection and Ranging techniques were actually already in use before the invention of the laser (at the time using flash lamps). Today lidars use state-of-the-art pulsed (but also continuous wave) lasers being emitted into the atmosphere. These short pulses are backscattered by both air molecules and suspended aerosols. The many different aspects of interaction of light and matter, from Rayleigh, Brillouin, Raman and Mie scattering over depolarization to absorption, give rise to numerous applications in atmospheric physics. Since even the shortest overview of these is already out of the scope of this chapter but may be found in books like Schumann (2012), Weitkamp (2005), and Measures (1984), the following paragraphs shall mention the techniques that possibly may contribute to turbulence detection and characterization. The next section will then describe the techniques relevant to the present aeronautics application in more detail.

Due to the numerous scattering processes, lidar technology may deliver information to nearly all observables indicative of turbulence, as described in Sect. 22.3. To start with, wind speed fluctuations along the line of sight $u'_{mol}(R)$ or its magnitude $\sigma^2_{u'_{mol}}(R)$, directly retrieved from air molecules backscatter, may be measured by determining the Doppler shift in the backscattered signal with interferometric methods. This approach, widely employed in airborne atmospheric research and in preparation for a European satellite mission, is explained in more detail in Sect. 22.5.2. As will be shown in Sect. 22.5.3, the vertical wind speed fluctuations present in clear-air turbulence should be accessible with an indirect method that relies on the adiabatic temperature changes of the air masses being turbulently stirred vertically. As mentioned in Sect. 22.3, the lateral wind v' renounces any measurement, "even" by lidar.

Coherent Doppler wind lidar is a widely used remote sensing technique for determining wind speeds. It is based on the determination of Doppler shift by heterodyne mixing of the narrow spectral line backscattered by aerosols suspended in the turbulent air flow. This technique thus delivers $u'_{aer}(R)$ and $\sigma^2_{u'_{aer}}(R)$. Some more details on this method are given in Sect. 22.5.1. Since it is based on

backscatter from aerosols, this method is applicable in regions of sufficient aerosol concentration (or more precisely effective backscatter cross-section). When this is the case, however, it allows a very convenient way of speed measurement along the line of sight.

Both coherent and interferometric methods allow derivation of three-dimensional wind vectors from a certain number of short-range measurements in different directions. Such a setup may thus be designed to provide information about turbulence ahead for input to an automated flight (attitude and lift) control system.

Section 22.3 above noted the air state variables as an important indicator of a turbulent motion of the air. Thus, temperature dispersion measurement with lidar should give the required information. On one hand, lidar technology offers different approaches for the remote measurement of air temperature. The analysis of the signal from different rotational Raman backscatter lines, for instance, allows a powerful technique for temperature determination, without being subject to atmospheric transmission (and thus, e.g., aerosol loading) (Behrendt 2005). Other techniques include the interferometric analysis of the backscattered Rayleigh-Brillouin line itself (Witschas et al. 2014), or the exploiting of the temperature dependence of molecular absorption (DIAL, differential absorption lidar) (Theopold and Bösenberg 1993). However, all these techniques require long integration times (minutes to hours) and rather long range-bins for averaging. This inhibits the measurement of short-scale fluctuations of the temperature $\sigma_T(R)$ as occurring in turbulent events. Moreover, for most Raman approaches daytime operation is not possible. While the temperature distribution (over range) is an important parameter for the understanding of the occurrence of turbulence, the previously mentioned methods do not promise to be applicable for the remote detection of turbulence itself.

The fluctuations of the optical air refractive index n_{opt}, generated by temperature fluctuations, have consequences on the propagation of the laser light: wavefront distortion with beam spread, beam wander, and scintillation. Zilberman and Kopeika (2004) operate a lidar similar to a scintillometer, deriving the refractive index structure constant from the variations of the angle of arrival of the backscatter "image" of the laser beam which is probing aerosol containing atmospheric layers. An application to horizontal airborne sensing is however negated by the resulting poor range resolution and the need for strong aerosol backscatter. More promising approaches have been proposed by Gurvich (2012) and Banakh and Smalikho (2011) relying on the backscatter enhancement effect. The methods employ an angular analysis of the total backscattered radiation, either by transmitting laser pulses in two angularly closely spaced regions or by employing two angularly separated detectors. While, to our knowledge, the proposed schemes have not yet been demonstrated in practice, the analytical considerations show a high potential for a real application (Gurvich 2014).

It was further conjectured that a passive tracer, such as aerosol or to a certain extent water vapor, may be useful for the lidar detection of turbulence in clear air. Among the earliest applications of lidar are the airborne investigations of CAT

relying on such a relationship between aerosol load variation and turbulence. Both the University of Michigan (Franken et al. 1966) and NASA (Lawrence et al. 1968; Melfi and Stickle 1969) have been performing flight tests into CAT areas with ruby laser-based lidar systems in the late 1960s. However, the found correlation between turbulence intensity (probed by the aircraft) and measured lidar backscatter variation was rather low in both cases, which was in part attributed to the limited achieved SNR of the systems (ibid.). Abandoned for decades (and replaced by studies with coherent Doppler systems), this relationship between aerosol backscatter fluctuation and turbulence structure -in particular on longitudinal scales- has recently found new interest. Zilberman et al. (2008) retrieve spectral characteristics from aerosol concentration measurements with ground-based lidar and allude to the complex relationship between the aerosol spatial spectrum and the spectrum of the underlying turbulence. Airborne water vapor measurements with lidar (Fischer et al. 2012) display variance spectra in general accordance with turbulence models, at least for the convective troposphere on rather large scales. These studies hint at the potential of passive tracer variance analysis for the determination of turbulence properties. The challenge is then to establish the relationship between the scalar's spectral characteristics and actual strength in terms of fluctuating wind speed.

The above noted observations on the interplay of turbulence sensing techniques and observables highlight the complexity of the underlying phenomenon. Turbulence acts on all dimensions and properties of the air, including the wind speeds relevant for an aircraft, and it generates variations in temperature and density due to these motions. The latter give rise to "optical turbulence," well known to astronomy and optical communication, that acts directly on electromagnetic waves (radio and optical alike). The turbulent air motion also disturbs regions formerly uniformly loaded with aerosols or other passive scalars. An inherent difficulty is represented by the complex relationships between these respective observables. This highlights the need for a deeper understanding and thus research concerning these relationships. Many of these phenomenological expressions of the underlying turbulence may be measured with photonic methods, from low radar frequencies to high ultraviolet laser radiation. As we have seen, probing with laser beams has the biggest potential with many different techniques. The most promising ones will be outlined in the next section.

The previous sections are brief summaries, and some techniques have been omitted due to obvious limitations (such as acoustic methods). Further reviews may be found in, admittedly dated, reviews of Collis (1966) and Atlas (1969).

22.5 Lidar Methods for Airborne Remote Detection of Turbulence

For lidar applications, there are two main approaches to determine the longitudinal wind speed, both relying on the Doppler shift of the backscattered light with respect to the emitted. While both the coherent and the direct detection technique may exploit the narrow backscatter from aerosols, the broad backscatter from air molecules may only be exploited by the direct detection technique. Figure 22.2 depicts a modeled backscatter from "typical" aerosol-laden air at different altitudes according to models. The return from air molecules is hereby broadened by its Brownian motion and thus a function of its temperature. The spectrum's width backscattered from aerosols is only slightly broadened (as compared to the incoming laser line) due to the wind speed fluctuations prevailing in the sensed air volume.

Excellent overviews of the coherent and direct detection lidar techniques may be found in Werner (2005) and Reitebuch (2012); the next sections summarize the approaches and give examples of applications. The third section gives an introduction of an alternative approach aiming the vertical wind speed as the target observable.

22.5.1 Coherent Doppler Lidar

The coherent Doppler lidar exploits, as the name implies, the coherent nature of the optical wave by mixing the spectrally narrow aerosol backscatter (left panel in

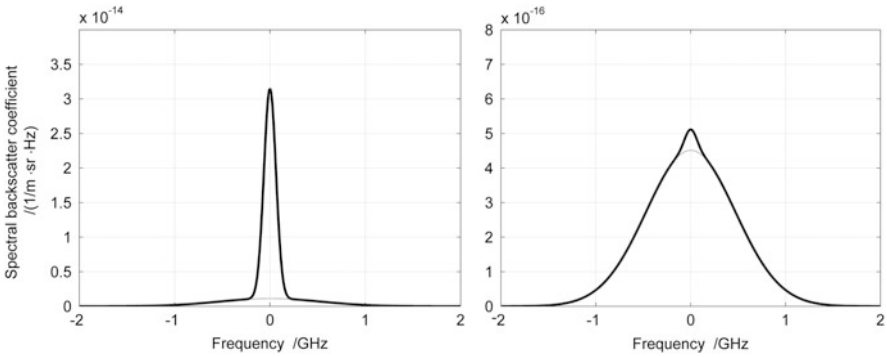

Fig. 22.2 Backscattered spectrum consisting of aerosol and molecular contribution, the latter (*thin lines*) Doppler-broadened due to air temperature. *Thick lines* show the combined spectral response. Two flight altitudes are shown: *left panel* for 500 m, *right panel* for 10,000 m, both for 532 nm irradiation. The lidar backscatter ratios are 3.2 and 0.018, respectively. Note the different scales for the backscatter coefficient [Derived with ESA Reference Atmosphere Model RMA (Vaughan et al. 1995; Vaughan et al. 1998)]

Fig. 22.2) to a local oscillator's optical wave on a fast detector. The frequency difference of the beat signal is then in the range of electronic detectors and circuits, and the Doppler shift may thus be deduced by a spectral analysis of the digitized signal (by Fourier transform, for instance). Further, the spectral width of this signal may be exploited in order to determine the turbulence intensity in terms of longitudinal wind speed variation within the sensed volume (e.g., Frehlich et al. 1998; Smalikho et al. 2005).

The following schematic (Fig. 22.3) depicts a simplified version of such a heterodyne detection lidar system.

The system employs both a pulsed or continuous-wave laser transmitter (LT) and a continuous-wave local oscillator (LO). The actual laser wavelength ν_0 is mainly chosen for a favorable ratio of aerosol to molecular backscatter coefficient, which are functions of wavelength. This aspect and also technological perspectives favor infrared systems with typical wavelengths 1.5–1.6 μm, 2 μm, and 10.6 μm depending on the laser technology. In the course of the development of coherent wind lidars, different laser types have and are being in use: from powerful CO_2 gas lasers over solid state to all fiber-based systems.

The laser LT and the reference laser LO are typically offset one from another by some intermediate frequency and locked with a phase lock loop (PLL). The remaining pulse-to-pulse frequency jitter is monitored by mixing the transmitted pulse with the LO on a reference detector DR. The laser pulse transmitted into the atmosphere is scattered within a range interval $c/2 \cdot \tau$ discriminated by the sample rate $1/\tau$ of the data acquisition's digitizer (for continuous-wave lasers, the focus of the transmit beam defines the single usable range gate). For the applications considered here (that emphasize measurement range), the laser radiation should be scattered from a sufficient number of particles in order to achieve an adequate heterodyne signal. The part scattered into the reverse direction is collected by a telescope, mixed with the LO and guided onto a detector (DA). Its output, similar to the reference DR's output, is subsequently digitized for spectrum analysis. From the shift $\Delta\nu_{aer}$ of the spectra of the atmospheric signal compared to the reference, one

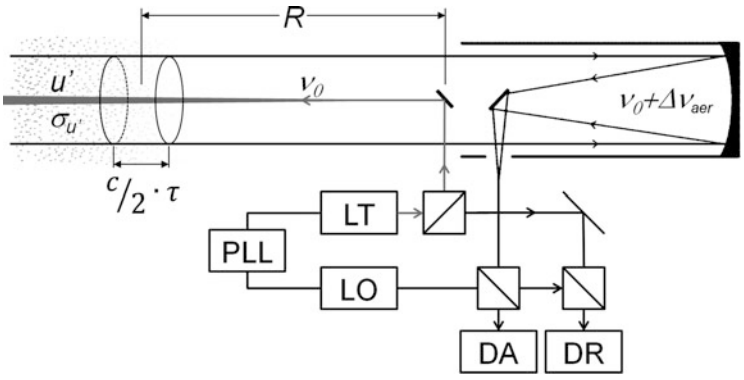

Fig. 22.3 Simplified synopsis of a coherent Doppler lidar. See text for abbreviations

may determine the axial Doppler wind fluctuation $u'_{\mathrm{aer}}(R)$ and from its spectral width retrieve information on the contained turbulence $\sigma^2_{u'_{\mathrm{aer}}}(R)$.

As mentioned, this coherent Doppler scheme may be implemented in various architectures covering near-range air data (true airspeed TAS), determination of the wind speed vector, measurement of wake vortices, and remote detection of clear-air turbulence.

The remote detection of CAT with lidar has long been pioneered by the USA, with activities undertaken by NASA and strong support from the FAA. The research activities on aerosol fluctuations (see above) have been followed by airborne tests of CO_2 coherent wind lidars (Weaver 1971; Huffaker 1975) on NASA's Convair aircraft in 1981 (Bilbro et al. 1984). Subsequent advancements in solid-state laser technology allowed simultaneous comparisons of such systems on NASA's B737 research aircraft in 1994 (Targ et al. 1996). The solid-state technology has been further evaluated by NCAR on the Electra aircraft during the ACLAIM program (Hannon et al. 1999; Soreide et al. 2000) in 1998, in collaboration with NASA. The ACLAIM lidar (build by CTI-Coherent Technologies Inc., now with Lockheed Martin) has further been tested on NASA's DC-8 aircraft within its WxAP project in 2003 (Teets et al. 2006). In 1999, the Japanese JAXA initiated a similar program for the development of an airborne coherent Doppler lidar. Prototypes of this fiber-based lidar system have been flown on JAXA's Beechcraft (for low altitudes research) in 2007 (Inokuchi et al. 2009) and its Gulfstream II aircraft in 2010 (Inokuchi et al. 2010; Inokuchi et al. 2014). All these flight tests of different coherent lidar systems show the high potential of this technology. In particular, wind speed accuracy has been determined to better than 1 m s^{-1}. Turbulence encounters were mostly very well correlated with significant axial wind speed deviations. The coherent systems exhibit a very good performance in low and medium altitudes where backscattering aerosols are abundant. However, for higher altitudes like the typical cruise levels of around 30–40 kft, the attained maximum range was limited throughout the experiments, i.e., too short for a timely turbulence warning. Teets et al. (2006) call for a "significant" increase in laser power for an adequate extension of warning time.

For shorter ranges, however, the ability to remotely detect spatially small phenomena like wake vortices has been demonstrated in an airborne vertical setup during the European AWIATOR project (Rahm et al. 2007) and in an airborne axial setup within the European I-Wake project (Douxchamps et al. 2008), both employing DLR's 2 μm wind lidar. This lidar is based on CTI's transceiver (Henderson et al. 1993; Köpp et al. 2004) and was operated on the German Aerospace Center's Falcon 20 aircraft and on the Dutch Aerospace Laboratory NLR's Cessna Citation 2 aircraft.

Generally, coherent wind lidar technology seems particularly well suited for near- to mid-range applications (of some tens to some hundred meters distance) where the backscatter signal even from low aerosol levels is still sufficient for an adequate signal-to-noise ratio. Accordingly, numerous systems are being developed, often with a focus on reducing size and ruggedizing the setup which favors fiber-based systems. Thus, the French Aerospace Laboratory ONERA has developed a series

of coherent lidar systems for near-range turbulence and wake vortex detection (Dolfi-Bouteyre et al. 2009). While the fiber-based technology seems a good candidate for airborne applications, a dedicated flight test campaign has not yet been performed.

Close detection of wake vortices may be used to feed an automated wake identification and alleviation system (Ehlers and Fezans 2015; Ehlers et al. 2015). Such a system then could generate control commands for rudders and lift control devices for counteracting the induced moments and lift forces. The necessary time constant here is dictated by the aircraft actuators, resulting in minimum ranges of around 50 m.

For closer applications, not explicitly covered here, such as the determination of (three-axis) true airspeed (TAS) very close to the fuselage of aircraft or helicopters, coherent Doppler lidar technology appears the method of choice. Some examples of the multitude of activities are the developments of THALES Avionics within the projects NESLIE and DANIELA (Verbeke 2010), JAXA's trial of a helicopter system (Matayoshi et al. 2007), and NCAR's development of an air motion sensor for its HIAPER Gulfstream GV research aircraft (Keeler et al. 1987; Spuler et al. 2011).

22.5.2 Direct Detection Doppler Lidar

As alluded to above, coherent Doppler lidar falls short whenever the aerosol concentration is too low to deliver sufficient backscatter signal-to-noise ratio at the distance of choice. Since the recovered radiation drops with more than the square of the distance, such conditions are usual at higher altitudes, which limits their use for long-range applications (such as turbulence warning), but also at shorter ranges. One way to overcome this difficulty is to determine the axial Doppler shift (or turbulent velocity distribution) from the spectrum of the *molecular* backscatter as opposed to *aerosol* backscatter. Since molecular backscatter is substantially broadened, as compared to a narrow laser line, by the temperature motion of the air (see Fig. 22.2), a heterodyne mixing is not exploitable for realistic pulse powers (Cézard 2008). A shift of this broad backscattered Rayleigh-Brillouin (RB) spectrum, though, may be determined using optical interferometry. Roughly speaking, the frequency information is converted into spatial (or rather angular) information when the received optical wave is brought to interference with itself. The output of the interferometer may then be analyzed radiometrically or spatially in order to derive the associated frequency shift. Accordingly, there exist two main approaches: the edge (or filter) technique and the fringe imaging technique. Actually, both methods also work for the narrow aerosol backscatter, but the optimum design differs depending on the proportion of the respective signals.

Figure 22.4 shows a synopsis of this "direct detection"-type lidar which is very similar for the transmission part and differs for the type of receiver implementation. A pulsed laser LT emits pulses into the atmosphere; in order to maximize the

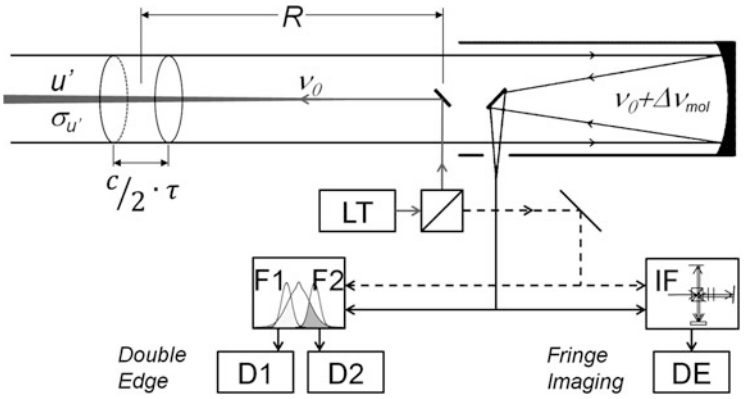

Fig. 22.4 Simplified synopsis of direct detection lidar with *left* double-edge receiver and *right* fringe imaging receiver. See text for abbreviations

backscatter signal, the laser radiation is often converted to ultraviolet wavelengths in order to profit from the high molecular backscatter. The backscattered radiation is collected by a telescope and brought on the receiver setup.

The edge technique (Flesia and Korb 1999) is based on a setup of (at least) two narrow spectral filters (F1 and F2) that are each centered in the flanks of the Rayleigh-Brillouin spectrum as depicted in Fig. 22.2. Part of this spectrum is transmitted through these filters, brought onto two detectors (D1 and D2) and digitized. The Doppler shift $\Delta\nu_{\mathrm{mol}}$ is then derived from the ratio of these two detector signals. This technique may also be implemented with more than two filters, with comparable performance (McGill and Spinhirne 1998). For a large number of filters, this technique basically transitions into the fringe imaging technique (see below). The other extreme is an implementation with only one filter which is also possible and may be realized by implementing an absorptive filter (Liu et al. 2007) (instead of an interference filter). The edge technique has been successfully applied in airborne applications, such as NASA's TWiLiTE lidar, which is autonomously operating on high-altitude research aircraft and the Global Hawk (Gentry et al. 2006), or the airborne demonstrator for Europe's satellite wind lidar ADM-Aeolus (Reitebuch et al. 2009) that is regularly deployed aboard DLR's Falcon 20 aircraft. Though, it has not yet been applied to forward-looking aeronautics applications as discussed herein.

The fringe imaging technique converts, by interferometry, the frequency shift $\Delta\nu_{\mathrm{aer}}$ into an angular shift of the output of the used interferometer (IF). This output is then imaged onto a matrix or line detector (DE). The digitized output is then used for fitting a line-shape model and thus determining the frequency shift as compared to the reference. As for the edge technique, the interferometer has either to be highly stabilized or regularly evaluated by a reference laser beam, derived from the transmitter LT.

Different types of interferometers may be used, each with its own benefits and weaknesses: Bruneau et al. (2004) demonstrated a Mach-Zehnder as spectral analyzer, Cézard (2008) and Liu et al. (2012) a Michelson, whereas the ADM-Aeolus spaceborne instrument will use a Fizeau interferometer (for its aerosol channel). A very widely used device is the Fabry-Perot interferometer. In the European project AWIATOR, a short-range lidar has been tested in forward-pointing configuration for flight control application (Schmitt et al. 2006). The lidar is based on a high repetition rate (18 kHz) solid-state UV laser which is sent, alternatingly, into four directions in order to retrieve a three-dimensional gust vector. The backscattered radiation is collected and fed through a Fabry-Perot etalon, its output intensified and imaged onto a CCD detector. The circular fringe pattern is then analyzed for the radius change due to Doppler shift. During the flight tests on Airbus' A340 test aircraft, wind speed dispersions of around 1.5 m s^{-1} at 50 m range for a flight altitude of 39 kft could be demonstrated (Rabadan et al. 2010), in line with the requirements of automatic control for gust load alleviation.

Whereas the Fabry-Perot etalon has clear advantages (high luminosity, ease of construction), it has the disadvantage of dispersing the received photons circularly on the detector; other interferometers can produce linear fringes (see Fig. 22.5). The latter may be imaged onto linear detector arrays by employing cylindrical lenses, thus enhancing the signal-to-noise ratio. The Fabry-Perot etalon eludes this possibility, thus requiring longer integration times. Optical workarounds have been proposed, such as circle-to-point converters (McGill et al. 1997), but these have other complications.

Generally, direct detection lidar seems a worthy alternative to coherent systems for short-range applications (such as for automatic control), offering the flexibility to operate within aerosol-laden as well as in aerosol-devoid altitudes and conditions.

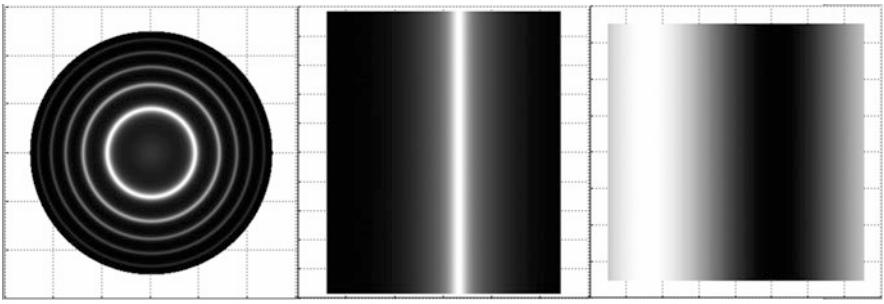

Fig. 22.5 Simulated interference patterns for Fabry-Perot, Fizeau, and Michelson interferometers (*left* to *right*, respectively). The Doppler shift results in a radial or linear shift of the imaged fringe, orders of magnitude smaller than the fringe width itself (around 5 MHz per m/s wind speed compared to the RB spectrum width of 1.7 GHz for UV wavelength at 10 km altitude)

22.5.3 Air Density Method

Another interesting approach for detecting clear-air turbulence was proposed by Feneyrou et al. (2009). It gives access (albeit indirectly) to the vertical wind speed fluctuation $\sigma^2_{w'_{\text{mol}}}(R)$ by relying on the linkage between potential and kinetic energy within turbulence. The approach provides a useful relationship between vertical velocity and air temperature. Air masses stirred up and down within the turbulent region undergo adiabatic cooling and heating, thus temperature fluctuations. The relationship reads (Feneyrou et al. 2009):

$$\sigma_{w'} = \frac{g}{N} \cdot \left(\frac{\partial T_{\text{air}}}{T_{\text{air}}} \right) = \frac{g}{N} \cdot \left(\frac{\partial \rho_{\text{air}}}{\rho_{\text{air}}} \right) = \frac{g}{N} \cdot \left(\frac{\partial \beta_{\text{mol}}}{\beta_{\text{mol}}} \right)$$

with g the gravity acceleration and N the Brunt-Väisälä frequency. N remains between 0.01 and 0.014 rad s^{-1} for typical cruise flight altitudes (around tropopause) (Birner 2003) and may be derived from a numerical weather forecast or in situ during the ascent of the aircraft. The temperature fluctuation measurement $\sigma^2_T(R)$ exceeds the capability limits of lidar detection (see Sect. 22.4.3) but may be replaced by measurement of air density fluctuations $\sigma^2_{\rho_{\text{mol}}}(R)$, which in turn may be determined by the air molecular backscatter fluctuation $\sigma^2_{\beta_{\text{mol}}}(R)$. However, these fluctuations are very minute, amounting to less than the 1 % level. Hence, any aerosol presence hampers this approach because its own backscatter signal may generate sufficient noise to mask the turbulent molecular variability. In order to exploit the stronger molecular backscatter (as with direct detection techniques), such a lidar should operate in the UV region. For an altitude of ≈10,000 m, a typical UV lidar backscatter ratio between aerosol and molecules $\beta_{\text{aer}} / \beta_{\text{mol}}$ amounts to less than 8×10^{-3} most of the time, according to Vaughan et al. (1995). However, this may not be expected to occur during all portions of cruise flight. Therefore, a high-resolution spectral filter should be employed in order to filter out the spectrally narrow aerosol return and use only the molecular wings of the RB spectrum.

The above approach has been tested within the French MMEDTAC project (Hauchecorne et al. 2010; Hauchecorne et al. 2016), relying on aerosol-devoid observation times. Within the European project DELICAT, the DLR built such a UV lidar for operation on the Dutch Cessna Citation 2 (Vrancken et al. 2010). Figure 22.6 depicts the possible layout of such a lidar system and the implementation within MMEDTAC and DELICAT.

A laser transmitter (LT) transmits powerful UV pulses into the atmosphere. The backscattered radiation is sent onto a very narrow spectral filter (SF), such as a Fabry-Perot etalon. In that case, both the transmitted and the reflected part of the spectrum are sent onto detectors DT and DR. Both outputs are used to perform an inversion in order to retrieve the purely molecular signal. Fluctuations of this backscatter may be analyzed by its variance or more advanced methods in order to determine the vertical wind speed fluctuation $\sigma^2_{w'_{\text{mol}}}(R)$. The DELICAT instrument

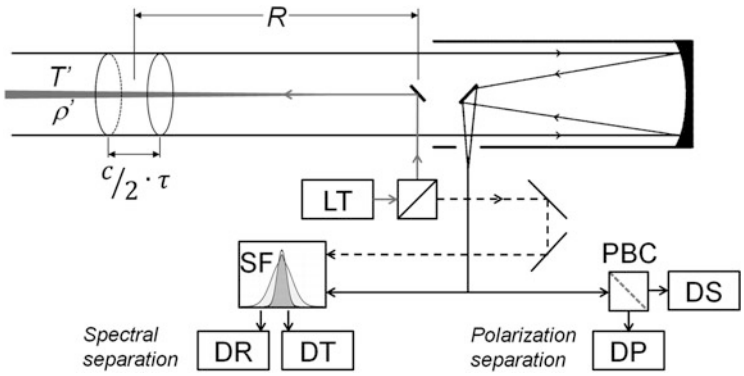

Fig. 22.6 Simplified synopsis of CAT lidar relying on density fluctuations. On the *left* employing spectral separation, on the *right* polarization separation as implemented within the DELICAT project. See text for abbreviations

employed, for these first airborne trials, a polarization separation assembly instead of the spectral filters. A good portion of the aerosols at these altitudes are represented by strongly depolarizing cirrus ice crystals which allow an exclusion of invalid data. Further, the flight campaign was planned according to aerosol content forecasted below a certain threshold. The flight campaign was executed in 2013 (Veerman et al. 2014) and demonstrated that the lidar is able to measure the molecular signal with a dispersion of better than 5×10^{-3} at distances between 10 and 15 km ahead (Vrancken et al. 2015). This allows the resolution of minute density fluctuations from moderate or greater turbulence severity. The instrumentation is subject of evolution within a DLR internal project in order to undergo further flight testing in the future.

This air density approach has the advantage of delivering the turbulence observable that is the most significant to aviation, viz., the vertical wind speed fluctuation $\sigma^2_{w',\mathrm{mol}}(R)$. Even with a noisy signal, and with the uncertainty on the stratification stability N, the derived quantity may be considered a qualified estimator of relevant turbulence intensity as compared to horizontal wind speed derived with Doppler wind lidars.

22.6 The Future

The previous sections highlight the inherent challenge of remote detection and characterization of a phenomenon as complex and capricious as turbulence. Turbulence occurring in clear and clean air, thus comprising CAT, MTW, NCT, and LLT, eludes detection with classical devices like radar. Passive remote sensing instruments, from radio to optical frequencies do not fulfill the tough requirements imposed by the aeronautics applications. Distant detection and near-range

quantification (in terms of wind speed) may only be attained by active optical remote sensing, i.e., lidar. Different approaches have been identified and the most important emphasized: the coherent Doppler wind lidar delivering the axial (thus horizontal) speed of aerosols embedded in the turbulent flow, $u'_{\mathrm{aer}}(R)$ and $\sigma^2_{u'_{\mathrm{aer}}}(R)$; the direct detection Doppler wind lidar that provides the axial speed of the air itself, $u'_{\mathrm{mol}}(R)$ and $\sigma^2_{u'_{\mathrm{mol}}}(R)$; and the indirect density method that gives vertical wind speed fluctuation $\sigma^2_{w'_{\mathrm{mol}}}(R)$. One should further mention the potential of passive tracer (i.e., aerosol) structuring and the backscatter enhancement effect that should be explored further. It seems that identifying the optimum instrumentation approach appears (nearly) as difficult as understanding turbulence itself!

Coherent Doppler lidars may be limited in their range due to the low aerosol density typical of normal cruising altitudes. On the other hand, situations with high aerosol content may constrain the density approach. The relationship between the horizontal wind speed and the more important vertical wind speed is not straightforward due to the anisotropy of stratified turbulence. The connection of optical turbulence (refractive index fluctuations) to wind velocity turbulence is even more uncertain. Eye safety issues impede the use of visual and near-visual (as UV and NIR) wavelengths while favoring infrared wavelengths.

In practice, it is worth considering whether a realistic airborne system should be comprised of different technologies or a consolidated method. What about function integration of other hazard detection, such as icing conditions, mineral dust, and volcanic ash? These are the questions that should be answered in the near future by the ongoing instrument and flight testing research.

One thing is for certain, turbulence occurring outside of clouds will remain detectable only with active optical means. Thus, the solution that addresses the issues of air safety, efficiency, and competitiveness in the context of turbulence will be lidar technology of the twenty-first century.

Acknowledgments The author would like to thank Oliver Reitebuch, Todd Lane, and Robert Sharman for the kind review of the present text.

References

Atlas, D.: Clear air turbulence detection methods: a review. In: Pao, Y.-H., Goldburg, A. (eds.) Clear Air Turbulence and Its Detection, pp. 381–401. Plenum Press, New York, NY (1969)

Atlas, D., Hardy, K.R., Naito, K.: Optimizing the radar detection of clear air turbulence. J. Appl. Meteorol. **5**(4), 450–460 (1966)

Banakh, V.A., Smalikho, I.N.: Determination of optical turbulence intensity by atmospheric backscattering of laser radiation. Atmos. Oceanic Opt. **24**(5), 457–465 (2011)

Baynes, J.: Rockwell Collins Unveils New MultiScan ThreatTrack™ Weather Radar. http://investor.rockwellcollins.com/investor-relations/press-releases/press-release-details/2014/Rockwell-Collins-Unveils-New-MultiScan-ThreatTrack-Weather-Radar (2014). Accessed 01 June 2015

Behrendt, A.: Temperature measurements with lidar. In: Weitkamp, C. (ed.) Lidar – Range-Resolved Optical Remote Sensing of the Atmosphere, pp. 273–305. Springer, New York, NY (2005)

Bilbro, J., Fichtl, G., Fitzjarrald, D., Krause, M., Lee, R.: Airborne Doppler lidar wind field measurements. Bull. Am. Meteorol. Soc. **65**(4), 348–359 (1984)

Birner, T.: Die extratropische Tropopausenregion. Dissertation, Ludwig-Maximilans-Universität, München (2003)

Bruneau, D., Garnier, A., Hertzog, A., Porteneuve, J.: Wind-velocity lidar measurements by use of a Mach–Zehnder interferometer, comparison with a Fabry–Perot interferometer. Appl. Opt. **43** (1), 173–182 (2004)

Buehler, W.E., King, C.H., Lunden, C.D.: Radar echoes from clear air inhomogeneities. In: Pao, Y.-H., Goldburg, A. (eds.) Clear Air Turbulence and Its Detection, pp. 425–435. Plenum Press, New York, NY (1969)

Cezard, N.: Etude de faisabilité d'un lidar Rayleigh-Mie pour des mesures à courte portée de la vitesse de l'air, de sa température et de sa densité. Dissertation, Ecole Polytechnique (2008)

Clifford, S.F., Kaimal, J.C., Lataitis, R.J., Strauch, R.G.: Ground-based remote profiling in atmospheric studies: an overview. Proc. IEEE **82**(3), 313–355 (1994)

Collis, R.T.H.: Clear air turbulence detection. Spectr. IEEE **3**(4), 56–61 (1966)

Crooks, W.M., Hoblit, F.M., Prophet, D.T., et al.: Project HICAT, An Investigation of High Altitude Clear Air Turbulence. Technical Report AFFDL-TR-67-123 Vol. 1, Air Force Flight Dynamics Laboratory (1967)

Dolfi-Bouteyre, A., Canat, G., Valla, M., Augere, B., Besson, C., Goular, D., Macq, B.: Pulsed 1.5-μm LIDAR for axial aircraft wake vortex detection based on high-brightness large-core fiber amplifier. IEEE J. Quantum Electron **15**(2), 441–450 (2009)

Douxchamps, D., Lugan, S., Verschueren, Y., Mutuel, L., Macq, B., Chihara, K.: On-board axial detection of wake vortices using a 2 μm LiDAR. IEEE Trans. Aerosp. Electron. Syst. **44**(4), 1276–1290 (2008)

Ehlers, J., Fezans, N.: Airborne doppler LiDAR sensor parameter analysis for wake vortex impact alleviation purposes. In Advances in Aerospace Guidance, Navigation and Control, pp. 433–453. Springer International Publishing (2015)

Ehlers, J., Fischenberg, D., Niedermeier, D.: Wake impact alleviation control based on wake identification. AIAA J. (2015). doi:10.2514/1.C033157

Feneyrou, P., Lehureau, J.-C., Barny, H.: Performance evaluation for long-range turbulence-detection using ultraviolet lidar. Appl. Opt. **48**(19), 3750–3759 (2009)

Fischer, L., Kiemle, Ch., Craig, G.C.: Height-resolved variability of midlatitude tropospheric water vapor measured by an airborne lidar. Geophys. Res. Lett. **39**(6), (2012). doi:10.1029/2011GL050621

Flesia, C., Korb, C.L.: Theory of the double-edge molecular technique for Doppler lidar wind measurement. Appl. Opt. **38**(3), 432–440 (1999)

Franken, P. A., Jenney, J. A., Rank, D. M.: Airborne investigations of clear air turbulence with laser radars (Clear air turbulence detection with laser radar, noting airborne equipment and results). In: 8th Annual Electron and Laser Beam Symposium, University of Michigan, Ann Arbor, pp. 87–103. (1966)

Frehlich, R., Hannon, S.M., Henderson, S.W.: Coherent Doppler lidar measurements of wind field statistics. Boundary-Layer Meteorol. **86**(2), 233–256 (1998)

Gentry, B., McGill, M., Schwemmer, G., Hardesty, M., Brewer, A., Wilkerson, Th., Lindemann, S.: The Tropospheric Wind Lidar Technology Experiment (TWiLiTE): An Airborne Direct Detection Doppler Lidar Instrument Development Program. Presentation to Earth Science Technology Conference, College Park (2006)

Good, R.E., Watkins, B.J., Quesada, A.F., Brown, J.H., Loriot, G.B.: Radar and optical measurements of Cn^2. Appl. Opt. **21**(18), 3373–3376 (1982)

Gurvich, A.S.: Lidar sounding of turbulence based on the backscatter enhancement effect. Izvestiya Atmos. Oceanic Phys. **48**(6), 585–594 (2012)

Gurvich, A.S.: Lidar positioning of higher clear-air turbulence regions. Izvestiya Atmos. Oceanic Phys. **50**(2), 143–151 (2014)

Haggerty, J., Schick, K., Mahoney, M.J., Lim, B.: The NCAR microwave temperature profiler: data applications from recent deployments. In: Microwave Radiometry and Remote Sensing of the Environment (MicroRad), pp. 133–135. 13th Specialist Meeting, Pasadena, CA (2014). doi:10.1109/MicroRad.2014.6878924

Hamilton, D.W., Proctor, F.H., Ahmad, N.N.: Flight Tests of the Turbulence Prediction and Warning System (TPAWS). NASA/TM-2012-217337 (2012)

Hannon, S.M., Bagley, H.R., Bogue, R.K.: Airborne Doppler lidar turbulence detection: ACLAIM flight test results. In: AeroSense'99, pp. 234–241. International Society for Optics and Photonics (1999)

Hauchecorne, A., Cot, Ch., Dalaudier, F., Porteneuve, J., Gaudo, Th., Wilson, R., Besson, C.: Set-up of a ground-based Rayleigh lidar to detect clear air turbulence. In: 25th International Laser Radar Conference (ILRC), pp. 269–272. St. Petersburg (2010)

Hauchecorne, A., Cot, C., Dalaudier, F., Porteneuve, J., Gaudo, T., Wilson, R., Cénac, C., Laqui, C., Keckhut, P., Perrin, J.-M., Dolfi, A., Cézard, N., Lombard, L., Besson, C.: Tentative detection of clear-air turbulence using a ground-based Rayleigh lidar. Appl. Opt. **55**(13), 3420–3428 (2016)

Henderson, S.W., Suni, P.J.M., Hale, C.P., Hannon, S.M., Magee, J.R., Bruns, D.L., Yuen, E.H.: Coherent laser radar at 2 μm using solid-state lasers. IEEE Trans. Geosci. Remote Sens. **31**(1), 4–15 (1993)

Hoblit, F.M.: Gust Loads on Aircraft: Concepts and Applications. AIAA Education Series. AIAA Inc., Washington, DC (1988)

Huffaker, R.M.: CO2 laser Doppler systems for the measurement of atmospheric winds and turbulence. Atmos. Technol. **1**, 71–76 (1975)

Inokuchi, H., Tanaka, H., Ando, T.: Development of an onboard doppler lidar for flight safety. J. Aircraft **46**(4), 1411–1415 (2009)

Inokuchi, H., Tanaka, H., Ando, T.: Development of a long range airborne Doppler LIDAR. In: Proceedings of 27th Congress of International Council of the Aeronautical Sciences (ICAS), **10** (3), (2010)

Inokuchi, H., Furuta, M., Inagaki, T.: High altitude turbulence detection using an airborne Doppler lidar. In: Proceedings of 29th Congress of the International Council of the Aeronautical Sciences (ICAS), St. Petersburg, 7–12 June 2014

Keeler, R.J., Serafin, R.J., Schwiesow, R.L., Lenschow, D.H., Vaughan, J.M., Woodfield, A.A.: An airborne laser air motion sensing system. Part I: Concept and preliminary experiment. J. Atmos. Oceanic Technol. **4**(1), 113–127 (1987)

Köpp, F., Rahm, S., Smalikho, I.: Characterization of aircraft wake vortices by 2 μm pulsed Doppler lidar. J. Atmos. Oceanic Technol. **21**(2), 194–206 (2004)

Lawrence Jr., J.D., McCormick, M.P., Melfi, S.H., Woodman, D.P.: Laser backscatter correlation with turbulent regions of the atmosphere. Appl. Phys. Lett. **12**(3), 72–73 (1968)

Lilly, D.K., Waco, D.E., Adelfang, S.I.: Stratospheric mixing estimated from high-altitude turbulence measurements. J. Appl. Meteorol. **13**(4), 488–493 (1973)

Liu, Z.S., Liu, B.Y., Li, Z.G., Yan, Z.A., Wu, S.H., Sun, Z.B.: Wind measurements with incoherent Doppler lidar based on iodine filters at night and day. Appl. Phys. B **88**(2), 327–335 (2007)

Liu, D., Hostetler, C., Miller, I., Cook, A., Hare, R., Harper, D., Hair, J.: Tilted pressure-tuned field-widened Michelson interferometer for high spectral resolution lidar. In SPIE Photonics Europe, pp. 84390P-84390P. International Society for Optics and Photonics, Apr (2012)

Luce, H., Nakamura, T., Yamamoto, M.K., Yamamoto, M., Fukao, S.: MU radar and lidar observations of clear-air turbulence underneath cirrus. Mon. Weather Rev. **138**(2), 438–452 (2010)

Matayoshi, N., Asaka, K., Okuno, Y.: Flight test evaluation of a helicopter airborne lidar. J. Aircraft **44**(5), 1712–1720 (2007)

McGill, M.J., Spinhirne, J.D.: Comparison of two direct-detection Doppler lidar techniques. Opt. Eng. **37**(10), 2675–2686 (1998)

McGill, M.J., Marzouk, M., Scott, V.S., Spinhirne, J.D.: Holographic circle-to-point converter with particular applications for lidar work. Opt. Eng. **36**(8), 2171–2175 (1997)
Measures, R.M.: Laser Remote Sensing: Fundamentals and Applications. Wiley, New York, NY (1984)
Melfi, S.H., Stickle, J.W.: Airborne laser-radar studies of the lower atmosphere. NASA-TN-D-5558 (1969)
Misaka, T., Holzäpfel, F., Hennemann, I., Gerz, T., Manhart, M., Schwertfirm, F.: Vortex bursting and tracer transport of a counter-rotating vortex pair. Phys. Fluids **24**(2), 025104 (2012)
Ottersten, H.: Atmospheric structure and radar backscattering in clear air. Rad. Sci. **4**(12), 1179–1193 (1969)
Rabadan, G.J., Schmitt, N.P., Pistner, T., Rehm, W.: Airborne lidar for automatic feedforward control of turbulent in-flight phenomena. J. Aircraft **47**(2), 392–403 (2010)
Rahm, S., Smalikho, I., Köpp, F.: Characterization of aircraft wake vortices by airborne coherent Doppler lidar. J. Aircraft **44**(3), 799–805 (2007)
Reitebuch, O.: Wind lidar for atmospheric research. In: Schumann, U. (ed.) Atmospheric Physics, pp. 487–507. Springer, Heidelberg (2012)
Reitebuch, O., Lemmerz, C., Nagel, E., Paffrath, U., Durand, Y., Endemann, M., et al.: The airborne demonstrator for the direct-detection Doppler wind lidar ALADIN on ADM-Aeolus. Part I: Instrument design and comparison to satellite instrument. J. Atmos. Oceanic Technol. **26**(12), 2501–2515 (2009)
Reiter, E.R., Burns, A.: The structure of clear-air turbulence derived from TOPCAT aircraft measurements. J. Atmos. Sci. **23**(2), 206–212 (1966)
Schaffner, Ph.R., Daniels, T.S., West, L.L., Gimmestad, G.G., Lane, S.E., Burdette, E.M., Sharman, R.D.: Experimental validation of a forward looking interferometer for detection of clear air turbulence due to mountain waves. In: 4th AIAA Atmospheric and Space Environments Conference, New Orleans (2012)
Schmitt, N., Rehm, W., Pistner, T., Zeller, P., Diehl, H., Navé, P.: Airborne direct detection UV lidar. In: Proceedings of 23rd International Laser Radar Conference, pp. 167–170. Nara, 24–28 July 2006
Schumann, U. (ed.): Atmospheric physics. Springer, Heidelberg (2012)
Serafimovich, A., Hoffmann, P., Peters, D., Lehmann, V.: Investigation of inertia-gravity waves in the upper troposphere/lower stratosphere over Northern Germany observed with collocated VHF/UHF radars. Atmos. Chem. Phys. **5**(2), 295–310 (2005)
Smalikho, I., Köpp, F., Rahm, S.: Measurement of atmospheric turbulence by 2 μm Doppler lidar. J. Atmos. Oceanic Technol. **22**(11), 1733–1747 (2005)
Soreide, D.C., Bogue, R.K., Ehernberger, J., Hannon, S.M., Bowdle, D.A.: Airborne coherent LIDAR for advanced in-flight measurements (ACLAIM) – flight testing of the LIDAR sensor. NASA-H-2428 (2000)
Spuler, S.M., Richter, D., Spowart, M.P., Rieken, K.: Optical fiber-based laser remote sensor for airborne measurement of wind velocity and turbulence. Appl. Optics **50**(6), 842–851 (2011)
Targ, R., Steakley, B.C., Hawley, J.G., Ames, L.L., Forney, P., Swanson, D., Robinson, P.A.: Coherent lidar airborne wind sensor II: Flight-test results at 2 and 10 μm. Appl. Opt. **35**(36), 7117–7127 (1996)
Teets Jr., E.H., Ashburn, C., Ehernberger, J., Bogue, R.: Turbulence and mountain wave conditions observed with an airborne 2-micron lidar. In: Remote Sensing, pp. 63670O. International Society for Optics and Photonics (2006)
Theopold, F.A., Bösenberg, J.: Differential absorption lidar measurements of atmospheric temperature profiles: theory and experiment. J. Atmos. Oceanic Technol. **10**(2), 165–179 (1993)
Vaughan, J.M., Brown, D.W., Nash, C., Alejandro, S.B., Koenig, G.G.: Atlantic atmospheric aerosol studies: 2. Compendium of airborne backscatter measurements at 10.6 μm. J. Geophys. Res. **100**(D1), 1043–1065 (1995)
Vaughan, J.M., Geddes, N.J., Flamant, P.H., Flesia, C.: Establishment of a backscatter coefficient and atmospheric database. ESA-CR12510 (1998)

Veerman, H.P., Vrancken, P., Lombard, L.: Flight testing DELICAT – a promise for medium-range clear air turbulence protection. In: Proceedings of the 25th SFTE European Chapter Symposium together with SETP European Section, Lulea, 15–18 June 2014

Verbeke, M.: LIDAR Airborne Aerodynamic Sensors – Thales Avionics. Presentation, In WAKENET-3 Europe/Greenwake Workshop, Palaiseau, 29–30 March 2010

Vernin, J., Pelon, J.: Scidar/lidar description of a gravity wave and associated turbulence: preliminary results. Appl. Opt. **25**(17), 2874–2877 (1986)

Vrancken, P., Wirth, M., Rempel, D., Ehret, G., Dolfi-Bouteyre, A., Lombard, L., Rondeau, Ph.: Clear air turbulence detection and characterisation in the DELICAT airborne lidar project. In: Proceedings of the 25th International Laser Radar Conference (ILRC), Saint Petersburg, 5–9 July 2010

Vrancken, P., Wirth, M., Ehret, G., Witschas, B., Veerman, H., Tump, R., Barny, H., Rondeau, Ph., Dolfi-Bouteyre, A., Lombard, L.: Flight tests of the DELICAT airborne LIDAR system for remote clear air turbulence detection. In: Proceedings of the 27th International Laser Radar Conference (ILRC), New York, 5–10 July 2015

Watkins, C.D., Browning, K.A.: The detection of clear air turbulence by radar. Phys. Technol. **4** (1), 28 (1973)

Weaver, E.A.: Clear-air-turbulence detection using lasers. Conf. Proc. NASA Aircraft Saf. Operating Prob. **1**, 89 (1971)

Werner, C.: Doppler wind lidar. In: Weitkamp, pp. 325–354 (2005)

Weitkamp, C. (ed.): Lidar: range-resolved optical remote sensing of the atmosphere. Springer, New York, NY (2005)

Witschas, B., Lemmerz, C., Reitebuch, O.: Daytime measurements of atmospheric temperature profiles (2–15 km) by lidar utilizing Rayleigh–Brillouin scattering. Opt. Lett. **39**(7), 1972–1975 (2014)

Zilberman, A., Kopeika, N.S.: LIDAR measurements of atmospheric turbulence vertical profiles. In Lasers and Applications in Science and Engineering, pp. 288–297. International Society for Optics and Photonics, June (2004)

Zilberman, A., Golbraikh, E., Kopeika, N.S., Virtser, A., Kupershmidt, I., Shtemler, Y.: Lidar study of aerosol turbulence characteristics in the troposphere: Kolmogorov and non-Kolmogorov turbulence. Atmos. Res. **88**(1), 66–77 (2008)